European Journal of Mechanics A/Solids 29 (2010) 591–599

Contents lists available at ScienceDirect

European Journal of Mechanics A/Solids

journal homepage: www.elsevier.com/locate/ejmsol

A micro scale Timoshenko beam model based on strain gradient elasticity theory

Binglei Wang, Junfeng Zhao, Shenjie Zhou*

School of Mechanical Engineering, Shandong University, Jingshi Road 73, Jinan 250061, Shandong, PR China

ARTICLE INFO

Article history:
Received 4 May 2009
Accepted 18 December 2009
Available online 6 January 2010

Keywords:
Micro scale
Timoshenko beam
Size effect
Strain gradient

ABSTRACT

A micro scale Timoshenko beam model is developed based on strain gradient elasticity theory. Governing equations, initial conditions and boundary conditions are derived simultaneously by using Hamilton's principle. The new model incorporated with Poisson effect contains three material length scale parameters and can consequently capture the size effect. This model can degenerate into the modified couple stress Timoshenko beam model or even the classical Timoshenko beam model if two or all material length scale parameters are taken to be zero respectively. In addition, the newly developed model recovers the micro scale Bernoulli–Euler beam model when shear deformation is ignored. To illustrate the new model, the static bending and free vibration problems of a simply supported micro scale Timoshenko beam are solved respectively. Numerical results reveal that the differences in the deflection, rotation and natural frequency predicted by the present model and the other two reduced Timoshenko models are large as the beam thickness is comparable to the material length scale parameter. These differences, however, are decreasing or even diminishing with the increase of the beam thickness. In addition, Poisson effect on the beam deflection, rotation and natural frequency possesses an interesting "extreme point" phenomenon, which is quite different from that predicted by the classical Timoshenko beam model.

1. Introduction

Micro scale beams are widely used in microstructure devices and systems such as sensors (Pei et al., 2004; Hall et al., 2006; Faris and Nayfeh, 2007; Moser and Gijs, 2007) and actuators (Hung and Senturia, 1999; De Boer et al., 2004), in which thickness of beams is typically on the order of microns and sub-microns. The size dependence of deformation behavior in micro scale beams had been experimentally observed in metals (Nix, 1989; Fleck et al., 1994; Poole et al., 1996), polymers (Lam and Chong, 1999; Lam et al., 2003; McFarland and Colton, 2005) and polysilicon (Chasiotis and Knauss, 2003). Due to lacking intrinsic length scales, conventional strain-based mechanical theories fail to interpret and predict such a size dependent phenomenon. Recently, higher-order continuum theories have been developed to predict these size dependences, in which strain gradient or nonlocal terms are involved and additional material length scale parameters are consequently introduced in addition to the classical material constants.

As one of the higher-order continuum theories, the classical couple stress elasticity theory, originated by Mindlin and Tiersten (1962), Mindlin (1964, 1965) and Toupin (1962), contains four material constants (two classical and two additional) for an isotropic elastic material. Some related research work has been performed to model the static and dynamic problems based on the classical couple stress elasticity theory (Zhou and Li, 2001; Kang and Xi, 2007). Based on the elastic theory, Yang et al. (2002) proposed a modified couple stress theory for elasticity by introducing the concept of the representative volume element, in which only symmetric rotation gradient tensor is considered and constitutive equations involve only one additional material length scale parameter besides two classical material constants. The theory had been applied to analyze static and dynamic problems of micro scale Bernoulli–Euler and Timoshenko beams (Park and Gao, 2006; Kong et al., 2008a; Ma et al., 2008).

Fleck and Hutchinson (1993, 1997, 2001) extended and reformulated the Mindlin's theory and renamed it the strain gradient theory, in which for homogeneous isotropic and incompressible materials, the second-order deformation gradient tensor is decomposed into two independent parts: the stretch gradient tensor and the rotation gradient tensor. In this formulation, conventional equilibrium relations are used and higher equilibrium conditions governing the behavior of higher-order stresses are ignored. As one of the most successful higher-order continuum theories, strain gradient elasticity theory proposed by Lam et al. (2003) introduces three material length scale parameters to characterize the dilatation gradient tensor, the deviatoric stretch gradient tensor and the symmetric rotation gradient tensor. The higher-order stress tensor work-conjugate to the new higher-order

* Corresponding author. Tel.: +86 531 88396708; fax: +86 531 88392700.
E-mail address: zhousj@sdu.edu.cn (S. Zhou).

0997-7538/$ – see front matter Crown Copyright © 2009 Published by Elsevier Masson SAS. All rights reserved.
doi:10.1016/j.euromechsol.2009.12.005

deformation metrics and the corresponding constitutive relations are defined. The theory has been used to analyze the static and dynamic problems of micro scale Bernoulli–Euler beam by Kong et al. (2008b). It should be noted that strain gradient elasticity theory of Lam et al. (2003) can degenerate into the modified couple stress theory of Yang et al. (2002) by setting two of the three material length scale parameters to be zero.

The size effect of Bernoulli–Euler beam model has also been studied by Tsepoura et al. (2002) and Papargyri-Beskou et al. (2003a,b). It should be noted that Papargyri-Beskou et al. (2003a,b) derived all possible boundary and initial conditions of the static and dynamic beam problems by variational principles. Papargyri-Beskou et al. (2003a,b) developed a higher-order Bernoulli–Euler beam model based on the gradient elasticity theory with surface energy of Vardoulakis and Sulem (1995), which involves four elastic constants (two classical and two non-classical). This strain gradient beam model has been explored further by Giannakopoulos and Stamoulis (2007), where the problems of bending of a cantilever beam and stretching of a cracked bar are analytically solved. The nonlocal continuum theory, suggested by Eringen (1983), is also used to predict the small scale effect by specifying the stress state at a given point to be a function of the strain states at all points in the body.

The classical Timoshenko beam theory, considering the effect of shear deformation, is used to model the short and stubby beam problems. Salvetat et al. (1999) mentioned that shear deformation in single-walled carbon nanotube rope becomes important when the ratio of length to radius is small. Some micro scale Timoshenko models have been developed via nonlocal continuum theory to study carbon nanotubes or other small beam-like members by Wang (2005), Wang et al. (2006, 2007), Lu et al. (2007), and Heireche et al. (2008). Ma et al. (2008) developed a microstructure-dependent Timoshenko beam model based on the modified couple stress theory due to Yang et al. (2002), which contains a material length scale parameter and can capture the size effect.

The object of this work is to develop a micro scale Timoshenko beam model by using both the basic equations of strain gradient elasticity theory and Hamilton's principle. The outline of this paper is organized as follows. In Section 2, the variational formulations of the micro scale Timoshenko beam based on the strain gradient elasticity theory are in detail deduced by using the Hamilton's principle. Then governing equations, initial conditions and all possible boundary conditions are obtained simultaneously. Subsequently, in Sections 3 and 4, the static bending and free vibration problems for a simple supported beam are solved respectively; corresponding numerical results for both problems are analyzed and discussed. Finally, some major conclusions are summarized in Section 5.

2. Model formulation

Compared to the modified couple stress theory of Yang et al. (2002), the strain gradient elasticity theory proposed by Lam et al. (2003) introduces additional dilatation gradient tensor and the deviatoric stretch gradient tensor in addition to the symmetric rotation gradient tensor. In order to characterize these tensors, there are three independent material length scale parameters in addition to two classical material constants for isotropic linear elastic materials. Then the strain energy U in a deformed isotropic linear elastic material occupying region Ω (with a volume element V) is given by

$$U = \frac{1}{2}\int_{\Omega}\left(\sigma_{ij}\varepsilon_{ij} + p_i\gamma_i + \tau^{(1)}_{ijk}\eta^{(1)}_{ijk} + m^s_{ij}\chi^s_{ij}\right)\mathrm{d}V \tag{1}$$

where the deformed measures: the strain tensor, ε_{ij}, the dilatation gradient tensor, γ_i, the deviatoric stretch gradient tensor, $\eta^{(1)}_{ijk}$, and the symmetric rotation gradient tensor, χ^s_{ij}, are defined by

$$\varepsilon_{ij} = \frac{1}{2}(\partial_j u_i + \partial_i u_j) \tag{2}$$

$$\gamma_i = \partial_i \varepsilon_{mm} \tag{3}$$

$$\eta^{(1)}_{ijk} = \eta^s_{ijk} - \frac{1}{5}\left(\delta_{ij}\eta^s_{mmk} + \delta_{jk}\eta^s_{mmi} + \delta_{ki}\eta^s_{mmj}\right) \tag{4}$$

and

$$\chi^s_{ij} = \frac{1}{4}(e_{ipq}\partial_p\varepsilon_{qj} + e_{jpq}\partial_p\varepsilon_{qi}) \tag{5}$$

where ∂_i is the differential operator, u_i is the displacement vector, ε_{mm} is the dilatation strain, and η^s_{ijk} is the symmetric part of second-order displacement gradient tensor defined by,

$$\eta^s_{ijk} = \frac{1}{3}\left(u_{i,jk} + u_{j,ki} + u_{k,ij}\right) \tag{6}$$

δ_{ij} and e_{ijk} are the Knocker symbol and the alternate symbol respectively. Here it should be noted that the index notation will always be used with repeated indices denoting summation from 1 to 3.

The stress measures: the classical stress tensor, σ_{ij}, and the higher-order stresses, p_i, $\tau^{(1)}_{ijk}$, and m^s_{ij}, are the work-conjugate to the deformation measures, given by

$$\sigma_{ij} = \frac{\partial w}{\partial \varepsilon_{ij}}, \quad p_i = \frac{\partial w}{\partial \gamma_i}, \quad \tau^{(1)}_{ijk} = \frac{\partial w}{\partial \eta^{(1)}_{ijk}}, \quad m^s_{ij} = \frac{\partial w}{\partial \chi^s_{ij}} \tag{7}$$

where the deformation energy density is a function of the strain and the higher-order deformations.

The corresponding stress measures, respectively, are given by the following constitutive relations,

$$\sigma_{ij} = k\delta_{ij}\varepsilon_{mm} + 2\mu\varepsilon'_{ij} \tag{8}$$

$$p_i = 2\mu l_0^2\gamma_i \tag{9}$$

$$\tau^{(1)}_{ijk} = 2\mu l_1^2\eta^{(1)}_{ijk} \tag{10}$$

$$m^s_{ij} = 2\mu l_2^2\chi^s_{ij} \tag{11}$$

where ε'_{ij} is the deviatoric strain defined as

$$\varepsilon'_{ij} = \varepsilon_{ij} - \frac{1}{3}\varepsilon_{mm}\delta_{ij} \tag{12}$$

k and μ are bulk and shear modules, respectively, l_0, l_1, and l_2 are the additional independent material length scale parameters associated with the dilatation gradients, deviatoric stretch gradients and symmetric rotation gradients respectively.

Consider a straight beam subjected to a static lateral load $q(x)$ distributed along the longitudinal axis x of the beam, as shown in Fig. 1. The loading plane coincides with the xz plane, and the cross-section of the beam parallels to the yz plane. The displacement fields in a Timoshenko beam can be described by (Dym and Shames, 1973)

$$\begin{aligned} u_1(x,y,z,t) &= -z\psi(x,t) \\ u_2(x,y,z,t) &= 0 \\ u_3(x,y,z,t) &= w(x,t) \end{aligned} \tag{13}$$

where

$$\psi(x,t) = \frac{\partial w(x,t)}{\partial x} - \beta(x,t) \tag{14}$$

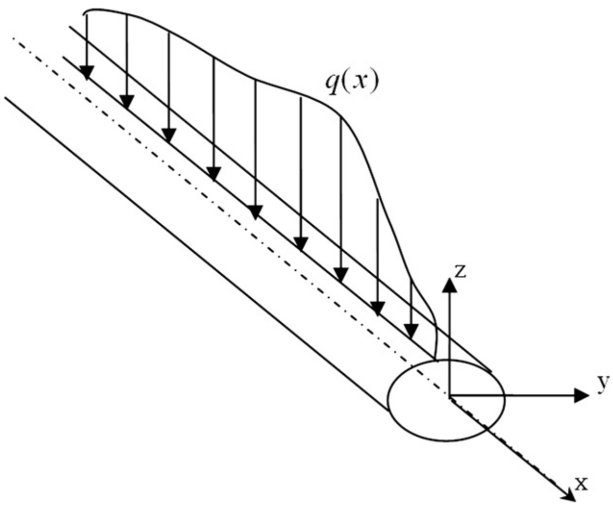

Fig. 1. Geometry and loading of the Timoshenko beam.

and t is time, $\psi(x,t)$ is the rotation of line elements along the centerline due to bending only; $\beta(x,t)$ is the rotation of line elements tangent to the centerline due to additional shear deformation. Here, we assume that the shear strain is the same at all points over a given cross-section of the beam. That is, the angle $\beta(x,t)$, used heretofore for rotation of elements along the centerline, is considered to measure the shear angle at all points in the cross-section of the beam at position x.

By substituting Eqs. (13) and (14) into Eq. (2), the non-zero strains ε_{ij} are

$$\varepsilon_{xx} = -z\left(\frac{\partial^2 w}{\partial x^2} - \frac{\partial \beta}{\partial x}\right)$$
$$\varepsilon_{xz} = \tfrac{1}{2}\beta \tag{15}$$

And from Eqs. (3) and (15), it follows that

$$\gamma_x = -z\left(\frac{\partial^3 w}{\partial x^3} - \frac{\partial^2 \beta}{\partial x^2}\right), \quad \gamma_y = 0, \quad \gamma_z = -\frac{\partial^2 w}{\partial x^2} + \frac{\partial \beta}{\partial x} \tag{16}$$

By inserting Eq. (15) into Eq. (5), the non-zero strain gradients χ^s_{ij} are

$$\chi^s_{xy} = \chi^s_{yx} = \frac{1}{4}\left(-2\frac{\partial^2 w}{\partial x^2} + \frac{\partial \beta}{\partial x}\right) \tag{17}$$

By using Eqs. (6) and (13), Eq. (4) gives

$$\begin{aligned}
&\eta^{(1)}_{111} = -\frac{2}{5}z\left(\frac{\partial^3 w}{\partial x^3} - \frac{\partial^2 \beta}{\partial x^2}\right), \quad \eta^{(1)}_{333} = \frac{1}{5}\left(\frac{\partial^2 w}{\partial x^2} - 2\frac{\partial \beta}{\partial x}\right)\\
&\eta^{(1)}_{113} = -\frac{4}{15}\left(\frac{\partial^2 w}{\partial x^2} - 2\frac{\partial \beta}{\partial x}\right), \quad \eta^{(1)}_{221} = \frac{1}{5}z\left(\frac{\partial^3 w}{\partial x^3} - \frac{\partial^2 \beta}{\partial x^2}\right)\\
&\eta^{(1)}_{223} = \frac{1}{15}\left(\frac{\partial^2 w}{\partial x^2} - 2\frac{\partial \beta}{\partial x}\right), \quad \eta^{(1)}_{331} = \frac{1}{5}z\left(\frac{\partial^3 w}{\partial x^3} - \frac{\partial^2 \beta}{\partial x^2}\right)\\
&\eta^{(1)}_{311} = \eta^{(1)}_{131} = -\frac{4}{15}\left(\frac{\partial^2 w}{\partial x^2} - 2\frac{\partial \beta}{\partial x}\right), \quad \eta^{(1)}_{322} = \eta^{(1)}_{232} = \frac{1}{15}\left(\frac{\partial^2 w}{\partial x^2} - 2\frac{\partial \beta}{\partial x}\right)\\
&\eta^{(1)}_{122} = \eta^{(1)}_{212} = \frac{1}{5}z\left(\frac{\partial^3 w}{\partial x^3} - \frac{\partial^2 \beta}{\partial x^2}\right), \quad \eta^{(1)}_{133} = \eta^{(1)}_{313} = \frac{1}{5}z\left(\frac{\partial^3 w}{\partial x^3} - \frac{\partial^2 \beta}{\partial x^2}\right)
\end{aligned} \tag{18}$$

From Eqs. (15) and (12) it follows that

$$\varepsilon'_{xx} = \frac{2}{3}\varepsilon_{xx}, \quad \varepsilon'_{yy} = \varepsilon'_{zz} = -\frac{1}{3}\varepsilon_{xx}, \quad \varepsilon'_{xz} = \varepsilon_{xz} = \frac{1}{2}\beta \tag{19}$$

The non-zero stresses σ_{ij} is obtained by substituting Eqs. (15) and (19) into Eq. (8)

$$\begin{aligned}
&\sigma_{xx} = -\left(k + \tfrac{4}{3}\mu\right)z\left(\frac{\partial^2 w}{dx^2} - \frac{\partial \beta}{dx}\right), \quad \sigma_{yy} = -\left(k - \frac{2}{3}\mu\right)z\left(\frac{\partial^2 w}{\partial x^2} - \frac{\partial \beta}{\partial x}\right)\\
&\sigma_{zz} = -\left(k - \tfrac{2}{3}\mu\right)z\left(\frac{\partial^2 w}{\partial x^2} - \frac{\partial \beta}{\partial x}\right), \quad \sigma_{xz} = \mu\beta
\end{aligned} \tag{20}$$

The last term in Eq. (20) indicates that the variation of σ_{xz} depends only on x. In order to account for the non-uniformity of the shear strain over the beam cross-section, a correction factor k_s, which varies with the shape of beam section, is introduced to the stress component σ_{xz} as follow (Hutchinson, 2001; Wang, 1995)

$$\sigma_{xz} = k_s\mu\beta \tag{21}$$

The use of Eq. (16) in Eq. (9) gives

$$\begin{aligned}
&p_x = -2\mu l_0^2 z\left(\frac{\partial^3 w}{\partial x^3} - \frac{\partial^2 \beta}{\partial x^2}\right), \quad p_y = 0,\\
&p_z = -2\mu l_0^2\left(\frac{\partial^2 w}{\partial x^2} - \frac{\partial \beta}{\partial x}\right)
\end{aligned} \tag{22}$$

And by inserting Eq. (17) into Eq. (11), the non-zero higher-order stresses m^s_{ij} are

$$m^s_{xy} = m^s_{yx} = \frac{1}{2}\mu l_2^2\left(-2\frac{\partial^2 w}{\partial x^2} + \frac{\partial \beta}{\partial x}\right) \tag{23}$$

Similarly, substituting Eq. (18) into Eq. (10), the non-zero higher-order stresses $\tau^{(1)}_{ijk}$ are

$$\begin{aligned}
&\tau^{(1)}_{111} = -\frac{4}{5}\mu l_1^2 z\left(\frac{\partial^3 w}{\partial x^3} - \frac{\partial^2 \beta}{\partial x^2}\right), \tau^{(1)}_{333} = \frac{2}{5}\mu l_1^2\left(\frac{\partial^2 w}{\partial x^2} - 2\frac{\partial \beta}{\partial x}\right)\\
&\tau^{(1)}_{113} = -\frac{8}{15}\mu l_1^2\left(\frac{\partial^2 w}{\partial x^2} - 2\frac{\partial \beta}{\partial x}\right), \tau^{(1)}_{221} = \frac{2}{5}\mu l_1^2 z\left(\frac{\partial^3 w}{\partial x^3} - \frac{\partial^2 \beta}{\partial x^2}\right)\\
&\tau^{(1)}_{223} = \frac{2}{15}\mu l_1^2\left(\frac{\partial^2 w}{\partial x^2} - 2\frac{\partial \beta}{\partial x}\right), \tau^{(1)}_{331} = \frac{2}{5}\mu l_1^2 z\left(\frac{\partial^3 w}{\partial x^3} - \frac{\partial^2 \beta}{\partial x^2}\right)\\
&\tau^{(1)}_{311} = \tau^{(1)}_{131} = -\frac{8}{15}\mu l_1^2\left(\frac{\partial^2 w}{\partial x^2} - 2\frac{\partial \beta}{\partial x}\right), \tau^{(1)}_{322} = \tau^{(1)}_{232} = \frac{2}{15}\mu l_1^2\left(\frac{\partial^2 w}{\partial x^2} - 2\frac{\partial \beta}{\partial x}\right)\\
&\tau^{(1)}_{122} = \tau^{(1)}_{212} = \frac{2}{5}\mu l_1^2 z\left(\frac{\partial^3 w}{\partial x^3} - \frac{\partial^2 \beta}{\partial x^2}\right), \tau^{(1)}_{133} = \tau^{(1)}_{313} = \frac{2}{5}\mu l_1^2 z\left(\frac{\partial^3 w}{\partial x^3} - \frac{\partial^2 \beta}{\partial x^2}\right)
\end{aligned} \tag{24}$$

By substituting Eqs. (15)–(18) and (20)–(24) into Eq. (1) and with the help of Eq. (14), the strain energy U is rewritten as

$$\begin{aligned}
U &= \frac{1}{2}\int_0^L \Big[k_1(w''' - \beta'')^2 + k_2(w'' - \beta')^2 + k_3(2w'' - \beta')^2\\
&\quad + k_4(w'' - 2\beta')^2 + k_5\beta^2\Big]dx\\
&= \frac{1}{2}\int_0^L \Big[k_1\psi''^2 + k_2\psi'^2 + k_3(w'' + \psi')^2 + k_4(-w'' + 2\psi')^2\\
&\quad + k_5(w' - \psi)^2\Big]dx
\end{aligned} \tag{25}$$

where

$$
\begin{aligned}
k_1 &= I\left(2\mu l_0^2 + \tfrac{4}{5}\mu l_1^2\right), \quad k_2 = I(k + \tfrac{4}{3}\mu) + 2\mu A l_0^2 \\
k_3 &= \frac{1}{4}\mu A l_2^2, \quad k_4 = \frac{8}{15}\mu A l_1^2, \quad k_5 = k_s \mu A
\end{aligned}
\tag{26}
$$

and $I = I_y = \int_A z^2 \, dA$ is the inertia moment of the beam, A and L are the cross-section area and the length of the beam respectively. The prime indicates partial derivative with respect to x.

From Eq. (25), the first variant of the strain energy U takes the following form,

$$
\begin{aligned}
\delta U = & \int_0^L \left[(k_3 + k_4)w^{IV} + (k_3 - 2k_4)\psi''' - k_5(w'' - \psi')\right]\delta w \mathrm{d}x \\
& + \int_0^L \left[k_1\psi^{IV} - (k_3 - 2k_4)w''' - (k_2 + k_3 + 4k_4)\psi''\right. \\
& \left. - k_5(w' - \psi)\right]\delta\psi \, \mathrm{d}x \quad + \left[-(k_3 + k_4)w''' - (k_3 - 2k_4)\psi''\right. \\
& \left. + k_5(w' - \psi)\right]\delta w\Big|_0^L + \left[(k_3 + k_4)w'' + (k_3 - 2k_4)\psi'\right]\delta w'\Big|_0^L \\
& + \left[-k_1\psi''' + (k_3 - 2k_4)w'' + (k_2 + k_3 + 4k_4)\psi'\right]\delta\psi\Big|_0^L \\
& + (k_1\psi'')\delta\psi'\Big|_0^L
\end{aligned}
\tag{27}
$$

where

$$
w^{IV} = \frac{\partial^4 w}{\partial x^4}, \quad \psi^{IV} = \frac{\partial^4 \psi}{\partial x^4}
\tag{28}
$$

On the other hand, the first variant of kinetic energy of the beam has the form

$$
\begin{aligned}
\delta T &= \delta \int_V \frac{1}{2}\rho\left[\left(\frac{\partial u_1}{\partial t}\right)^2 + \left(\frac{\partial u_2}{\partial t}\right)^2 + \left(\frac{\partial u_3}{\partial t}\right)^2\right]\mathrm{d}v \\
&= \rho \int_0^L \left(A\dot{w}\delta\dot{w} + I\dot{\psi}\delta\dot{\psi}\right)\mathrm{d}x
\end{aligned}
\tag{29}
$$

where ρ is the material density, and a superimposed dot indicates the time derivative.

Then the first variations of the work done by the external force $q(x)$, the boundary shear force V and the boundary classical and double moments M and M_h, respectively, read

$$
\delta W = \int_0^L q(x)\delta w \, \mathrm{d}x + V\delta w\Big|_0^L + M\delta w'\Big|_0^L + M_h\delta\psi'\Big|_0^L
\tag{30}
$$

According to Hamilton's principle, the actual motion minimizes the difference of the kinetic energy and total potential energy for a system with prescribed configurations at t_1 and t_2. That is

$$
\delta \int_{t_1}^{t_2} [T - (U - W)]\mathrm{d}t = 0
\tag{31}
$$

Substituting Eqs. (27), (29) and (30) into Eq. (31), it takes the form as

$$
\begin{aligned}
& \int_{t_1}^{t_2}\int_0^L -\rho A\ddot{w} + q - \left[(k_3 + k_4)w^{IV} + (k_3 - 2k_4)\psi'''\right. \\
& \left. - k_5(w'' - \psi')\right]\delta w \, \mathrm{d}x \, \mathrm{d}t \quad + \int_{t_1}^{t_2}\int_0^L -\rho I\ddot{\psi} - \left[k_1\psi^{IV} - (k_3 - 2k_4)w'''\right. \\
& \left. - (k_2 + k_3 + 4k_4)\psi'' - k_5(w' - \psi)\right]\delta\psi \, \mathrm{d}x \, \mathrm{d}t \\
& + \int_0^L \rho A\dot{w}\delta w\Big|_{t_1}^{t_2}\mathrm{d}x + \int_0^L \rho I\dot{\psi}\delta\psi\Big|_{t_1}^{t_2}\mathrm{d}x - \int_{t_1}^{t_2}\left\{\left[-V - (k_3 + k_4)w'''\right.\right. \\
& \left.\left. - (k_3 - 2k_4)\psi'' + k_5(w' - \psi)\right]\delta w\Big|_0^L\right\}\mathrm{d}t \\
& - \int_{t_1}^{t_2}\left\{\left[-M + (k_3 + k_4)w'' + (k_3 - 2k_4)\psi'\right]\delta w'\Big|_0^L\right\}\mathrm{d}t \\
& - \int_{t_1}^{t_2}\left\{\left[-k_1\psi''' + (k_3 - 2k_4)w'' + (k_2 + k_3 + 4k_4)\psi'\right]\delta\psi\Big|_0^L\right\}\mathrm{d}t \\
& - \int_{t_1}^{t_2}\left[(-M_h + k_1\psi'')\delta\psi'\Big|_0^L\right]\mathrm{d}t = 0
\end{aligned}
\tag{32}
$$

Due to the fundamental lemma of the calculus of variation with the arbitrariness of δw and $\delta\psi$ for given $x \in [0, L]$ and $t \in [t_1, t_2]$, the governing equations (i.e. the Euler–Lagrange equations) of the beam in bending are given by

$$
\begin{aligned}
& \rho A\ddot{w} - q + (k_3 + k_4)w^{IV} + (k_3 - 2k_4)\psi''' - k_5(w'' - \psi') = 0 \\
& \rho I\ddot{\psi} + k_1\psi^{IV} - (k_3 - 2k_4)w''' - (k_2 + k_3 + 4k_4)\psi'' - k_5(w' - \psi) = 0
\end{aligned}
\tag{33}
$$

the initial conditions can be written as

$$
\begin{aligned}
& (\rho A\dot{w}\delta w)\Big|_{t_1}^{t_2} = 0 \\
& \left(\rho I\dot{\psi}\delta\psi\right)\Big|_{t_1}^{t_2} = 0
\end{aligned}
\tag{34}
$$

and the boundary conditions read,

$$
\begin{aligned}
& (k_3 + k_4)w''' + (k_3 - 2k_4)\psi'' - k_5(w' - \psi) = -\overline{V} \text{ or } \\
& \quad w = \overline{w} \text{ at } x = 0 \text{ and } x = L(k_3 + k_4)w'' + (k_3 - 2k_4)\psi' \\
& \quad\quad = \overline{M} \text{ or } w' = \overline{w}' \text{ at } x = 0 \text{ and } x = L - k_1\psi''' \\
& \quad\quad\quad + (k_3 - 2k_4)w'' + (k_2 + k_3 + 4k_4)\psi' = 0 \text{ or } \\
& \psi = \overline{\psi} \text{ at } x = 0 \text{ and } x = Lk_1\psi'' = \overline{M}_h \text{ or } \psi' = \overline{\psi}' \text{ at } x \\
& \quad = 0 \text{ and } x = L
\end{aligned}
\tag{35}
$$

where the overbar represents the prescribed value. Solving the governing equations (33) with the initial conditions of Eq. (34) and proper boundary conditions of Eq. (35), $w(x,t)$ and $\psi(x,t)$ will be determined.

It is clearly seen from Eqs. (33)–(35) that the present model contains three material length scale parameters (l_0, l_1 and l_2), which enables the model to predict the size effect. However, when the material length scale parameters l_0 and l_1 are equal to zero, the governing equations and boundary conditions will reduce to those of the modified couple stress model (Ma et al., 2008). Furthermore, if all the material length scale parameters l_0, l_1 and l_2 are equal to zero, the governing equations and boundary conditions will directly degenerate to those of the classical Timoshenko beam model. In addition, the governing equations and boundary conditions degenerate to those of the micro scale Bernoulli–Euler beam

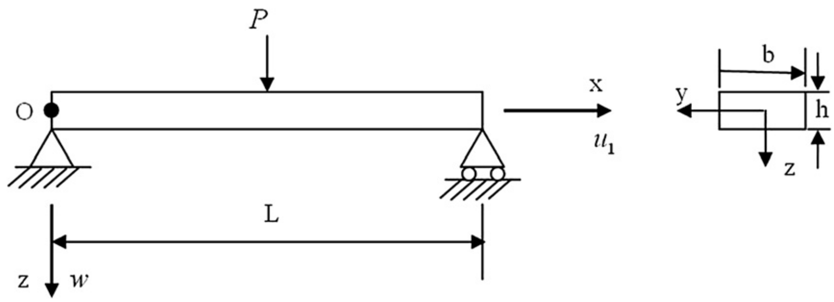

Fig. 2. Schematic figure of the simply supported beam.

model based on strain gradient elasticity theory when shear deformation is neglected (Kong et al., 2008b).

3. Static bending of a simply supported beam

Assuming a simply supported beam subjected to a concentrated force, as shown in Fig. 2, where the loading, geometry, and cross-sectional shape are also shown, the boundary conditions of the static bending problem can be simplified as (Ma et al., 2008)

$$w|_{x=0} = w|_{x=L} = 0, \quad w''|_{x=0} = w''|_{x=L} = 0, \quad \psi'|_{x=0} = \psi'|_{x=L} = 0 \tag{36}$$

For a static bending problem, the time derivatives are set to zero in Eq. (33) and then the governing equations for static problems are given by

$$\begin{aligned} (k_3+k_4)w^{IV} + (k_3-2k_4)\psi''' - k_5(w''-\psi') &= q \\ k_1\psi^{IV} - (k_3-2k_4)w''' - (k_2+k_3+4k_4)\psi'' - k_5(w'-\psi) &= 0 \end{aligned} \tag{37}$$

In order to derive the solutions, $w(x)$ and $\psi(x)$ can be expanded as the following Fourier series

$$w(x) = \sum_{n=1}^{\infty} W_n \sin\left(\frac{n\pi x}{L}\right), \quad \psi(x) = \sum_{n=1}^{\infty} \Phi_n \cos\left(\frac{n\pi x}{L}\right) \tag{38}$$

where W_n and Φ_n are Fourier coefficients to be determined for each n. It is obvious that the expansions in Eq. (38) satisfy the boundary conditions in Eq. (36) for any W_n and Φ_n.

Based on Eq. (38), the applied load $q(x)$ can also be expanded in a Fourier series as

$$q(x) = \sum_{n=1}^{\infty} Q_n \sin\left(\frac{n\pi x}{L}\right) \tag{39}$$

For a given $q(x)$, Q_n in Eq. (39) can be readily determined to be

$$Q_n = \frac{2}{L}\int_0^L q(x)\sin\left(\frac{n\pi x}{L}\right)\mathrm{d}x \tag{40}$$

In the present investigation as shown in Fig. 2, $q(x) = P\delta(x-L/2)$, where $\delta(\bullet)$ is the Dirac delta function and P is the concentrated force. Substituting $q(x)$ of Eq. (39) into Eq. (40), then it gives

$$Q_n = \frac{2}{L}P\sin\left(\frac{n\pi}{2}\right) \tag{41}$$

Substituting Eqs. (38) and (39) into Eq. (37) gives

$$\begin{bmatrix} \alpha^4(k_3+k_4)+\alpha^2k_5 & \alpha^3(k_3-2k_4)-\alpha k_5 \\ \alpha^3(k_3-2k_4)-\alpha k_5 & \alpha^4k_1+\alpha^2(k_2+k_3+4k_4)+k_5 \end{bmatrix}\begin{Bmatrix} W_n \\ \Phi_n \end{Bmatrix} = \begin{Bmatrix} Q_n \\ 0 \end{Bmatrix} \tag{42}$$

where $\alpha = n\pi L$.

Solving the above linear algorithm sets of Eq. (42), W_{n} and Φ_n can be determined as

$$\begin{aligned} W_n &= \frac{\alpha^4k_1+\alpha^2(k_2+k_3+4k_4)+k_5}{\left[\alpha^4(k_3+k_4)+\alpha^2k_5\right]\left[\alpha^4k_1+\alpha^2(k_2+k_3+4k_4)+k_5\right]-\left[\alpha^3(k_3-2k_4)-\alpha k_5\right]^2}Q_n \\ \Phi_n &= \frac{-\left(\alpha^3(k_3-2k_4)-\alpha k_5\right)}{\left[\alpha^4(k_3+k_4)+\alpha^2k_5\right]\left[\alpha^4k_1+\alpha^2(k_2+k_3+4k_4)+k_5\right]-\left[\alpha^3(k_3-2k_4)-\alpha k_5\right]^2}Q_n \end{aligned} \tag{43}$$

With W_n and Φ_n determined from Eq. (43), the analytical solutions of $w(x)$ and $\psi(x)$ for the static bending of the simply supported Timoshenko beam subjected to the concentrated force P are determined by substituting Eq. (43) into Eq. (38). After somewhat lengthy but straightforward manipulations, all other physical quantities can be subsequently determined without any difficulty.

Some numerical results have been obtained and presented in Figs. 3–6 to demonstrate the behavior of static bending of the micro scale Timoshenko beam subjected to a concentrated force. For the purpose of illustration, the beam considered here is taken to be made of epoxy with the following properties: the elastic modulus

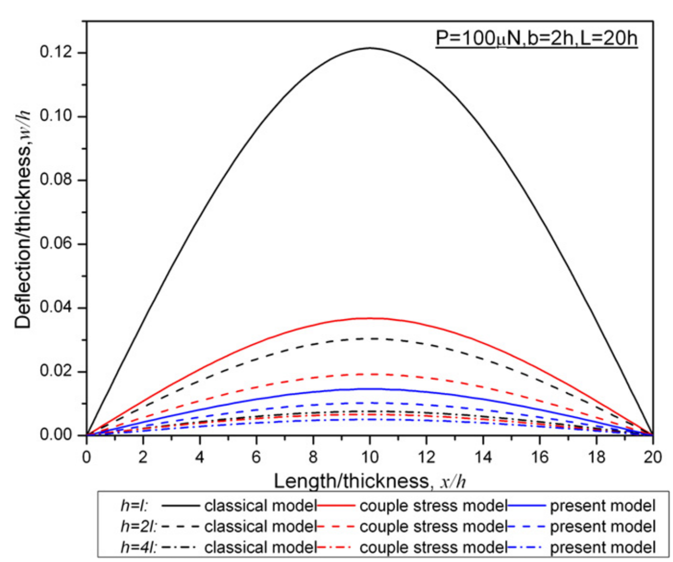

Fig. 3. Deflection of the simply supported Timoshenko beam based on three different models with $h = l$, $2l$, $4l$.

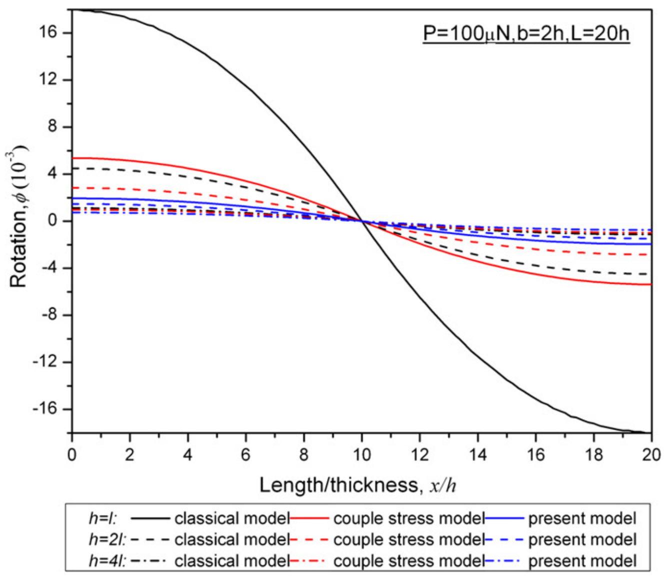

Fig. 4. Rotation of the simply supported Timoshenko beam based on three different models with $h = l$, $2l$, $4l$.

$E = 1.44$ GPa, the Poisson's ratio $\nu = 0.38$ and the material length scale parameter $l = 17.6$ μm (Lam et al., 2003). The cross-sectional shape is kept to be the same by letting $b/h = 2$ and the length of the beam is selected to be $L/h = 20$ for all cases, as shown in Fig. 2. The values of P and h are chosen in such a way that the beam remains elastic everywhere (Park and Gao, 2006; Ma et al., 2008). The shear coefficient of Timoshenko beam k_s is taken to be $(5+5\nu)/(6+5\nu)$, which was shown to be the best expression for a rectangular cross-section beam (Kaneko, 1975). For simplification, we assume that all three material length scale parameters are the same, i.e., $l_0 = l_1 = l_2 = l$ within the micro scale Timoshenko beam model. Numerical results for the present model are plotted in Figs. 3–6, in which those for the modified couple stress Timoshenko beam model ($l_0 = l_1 = 0$, $l_2 = l$) and the classical Timoshenko beam model ($l_0 = l_1 = l_2 = 0$) are also plotted.

Figs. 3 and 4 show the deflection $w(x)$ and the corresponding rotation $\psi(x)$ (due to bending only) for three sets of geometries of

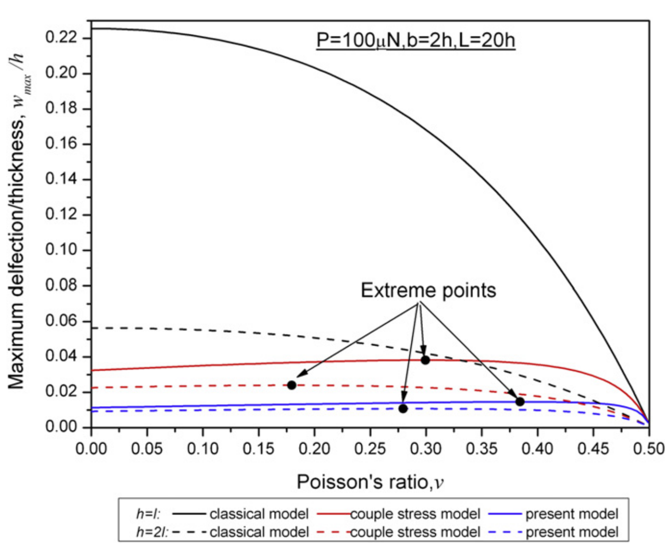

Fig. 5. Poisson effect on the maximum deflection of the Timoshenko beam based on three different models with $h = l$, $2l$.

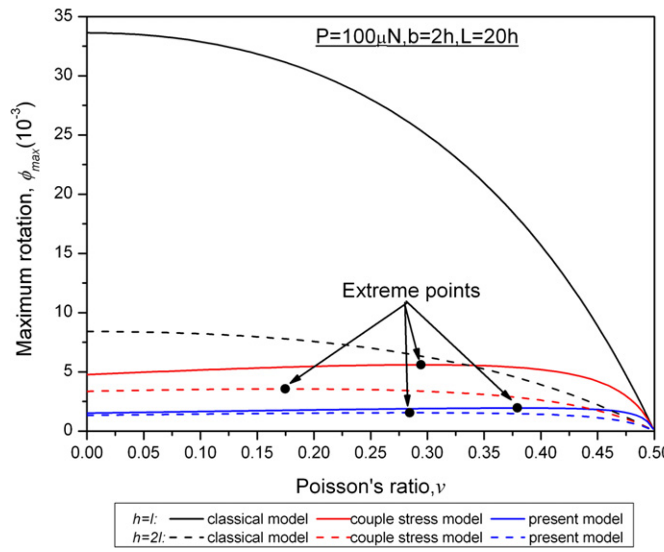

Fig. 6. Poisson effect on the maximum rotation of the Timoshenko beam based on three different models with $h = l$, $2l$.

the micro scale Timoshenko beam shown in Table 1. It is clearly observed from Fig. 3 that the deflection predicted by the present model is not only smaller than that by the classical model but also smaller than that by the modified couple stress model for three set of geometries. This indicates that the present model exhibits increased bending rigidity due to the fact that strain gradient elasticity theory introduces additional dilatation gradient tensor and the deviatoric stretch gradient tensor in addition to the symmetric rotation gradient tensor. The absolute values of the rotation for three models in Fig. 4 show the similar trend as shown in Fig. 3. Furthermore, it is seen from Figs. 3 and 4 that there are large differences in the deflection and rotation for the three different models when the beam thickness h is approximately equal to the material length scale length parameter (with $h = l = 17.6$ μm). However, such differences are decreasing or even diminishing as thickness of the beam becomes greater e.g., $h = 4l = 70.4$ μm. It indicates that the size effect is only significant when the beam thickness is comparable to the material length scale parameter. This agrees with what was observed experimentally (McFarland and Colton, 2005). So we can conclude that the increased stiffening effect for the static deformation is due to the microstructure, which is also observed in Papargyri-Beskou et al. (2003a,b).

For further observations on Poisson effect, the variable tendencies of maximum deflection and maximum rotation with Poisson ratio varying from 0 to 0.5 are quantitatively shown in Figs. 5 and 6 respectively. Both cases of beam thickness ($h = l$ and $h = 2l$) are considered. Fig. 5 illustrates that the maximum deflection predicted by the classical model decreases gradually with Poisson's ratio. However, there is a noticeable trend that the results predicted by the present model increase firstly and then decrease with Poisson's ratio increasing, which is quite different from that predicted by the classical model. Further investigations in Fig. 5 show that results predicted by the modified couple stress model exhibit

Table 1
Sets of geometries configurations for a micro scale Timoshenko beam.

Sets	1	2	3
Thickness, h (μm)	17.6	35.2	70.4
Width, $b = 2h$ (μm)	35.2	70.4	140.8
Length, $L = 20h$ (μm)	352.0	704.0	1408.0

the same trend as those by the present model. A similar phenomenon is also observed for the maximum rotation in Fig. 6. This variable tendency may be named as a maximum "extreme point" phenomenon, which is the result of the introduction of the material length scale parameters for the micro scale Timoshenko models. As typically micro scale models, both the present model and the modified couple stress model have extreme points for different beam thicknesses ($h=l$ and $h=2l$), while the classical model exhibits a monotonically decreasing trend with Poisson's ratio as shown in Figs. 5 and 6, indicating having no such 'extreme point' phenomenon.

4. Free vibration of a simply supported beam

For the free vibration problem of a simply supported beam shown in Fig. 2, the external force $q(x)$ in Eq. (33) vanishes and $V=0$, $M=0$ and $M_h=0$ in boundary conditions of Eq. (35). Similar to the procedure of static bending problem, the following Fourier series solutions for $w(x,t)$ and $\psi(x,t)$ are employed

$$w(x,t) = \sum_{n=1}^{\infty} W_n^{\mathrm{D}} \sin\left(\frac{n\pi x}{L}\right) e^{i\omega_n t}, \quad \psi(x,t) = \sum_{n=1}^{\infty} \Phi_n^{\mathrm{D}} \cos\left(\frac{n\pi x}{L}\right) e^{i\omega_n t} \tag{44}$$

where W_n^{D} and Φ_n^{D} are Fourier coefficients, the superscript "D" denotes dynamic problem, ω_n is the vibration frequency, and i is the usual imaginary number defined by $i^2=-1$. Similarly, the expansions in Eq. (44) satisfy the boundary conditions in Eq. (36) for any W_n^{D} and Φ_n^{D}.

Using the expansions in Eq. (44), the governing equations in Eq. (33) can be rewritten as

$$\begin{bmatrix} \alpha^4(k_3+k_4)+\alpha^2 k_5-\rho A\omega_n^2 & \alpha^3(k_3-2k_4)-\alpha k_5 \\ \alpha^3(k_3-2k_4)-\alpha k_5 & \alpha^4 k_1+\alpha^2(k_2+k_3+4k_4)+k_5-\rho I\omega_n^2 \end{bmatrix} \times \begin{Bmatrix} W_n^{\mathrm{D}} \\ \Phi_n^{\mathrm{D}} \end{Bmatrix} = 0 \tag{45}$$

For a non-trivial solution of W_n^{D} ($\neq 0$) and Φ_n^{D} ($\neq 0$), it is required that the determinant of the coefficient matrix of Eq. (45) vanishes, which leads to

$$e_1\omega_n^4+e_2\omega_n^2+e_3 = 0 \tag{46}$$

where

$$\begin{aligned} e_1 &= \rho^2 AI \\ e_2 &= -\rho I\left[\alpha^4(k_3+k_4)+\alpha^2 k_5\right]-\rho A\left[\alpha^4 k_1+\alpha^2(k_2+k_3+4k_4)+k_5\right] \\ e_3 &= \left[\alpha^4(k_3+k_4)+\alpha^2 k_5\right]\left[\alpha^4 k_1+\alpha^2(k_2+k_3+4k_4)+k_5\right] \\ &\quad -\left[\alpha^3(k_3-2k_4)-\alpha k_5\right]^2 \end{aligned} \tag{47}$$

The equation of ω_n^2 can be easily obtained by solving the quadratic Eq. (46),

$$\omega_n^2 = \frac{-e_2-\sqrt{e_2^2-2e_1e_3}}{2e_1} \tag{48}$$

which is the smaller of two roots for ω_n^2. The positive solution of ω_n determined from Eq. (48) is the natural frequency of the simply supported beam for different order number n. Once ω_n is determined, the Fourier coefficients ω_n^{D} and Φ_n^{D} will be obtained by Eq. (45) and $w(x)$ and $\psi(x)$ are further determined by Eq. (44). It should be noted that ω_n in Eq. (48) degenerates into the natural frequency predicted by the modified couple stress model by Ma et al. (2008) when two material length scale parameters equal to zero (i.e., $l_0=l_1=0$).

Fig. 7 shows how the first order natural frequency predicted by three Timoshenko beam models (the present model, the modified couple stress model and the classical model) change with dimensionless thickness of the beam (h/l) for different values of Poisson's ratio ($\nu=0.0$ and $\nu=0.38$). For the purpose of illustration, the beam considered here is also taken to be made of epoxy and material properties used in the calculations are the same as those in static bending problem, and material density is taken to be $\rho=1.22$ kg/m^3 (Maneschy et al., 1986).

For the microstructure, the increased stiffening effect for static problem can result in the increased natural frequency for the dynamic problem. It is seen from Fig. 7 that the natural frequency predicted by the present model is not only larger than that by the classical model but also larger than that by the modified couple stress model for two different values of Poisson's ratio especially when the beam thickness is approximately equal to the material length scale parameter. This is due to the increased bending rigidity introduced by the present model as shown in Fig. 3. Moreover, for both cases of $\nu=0.0$ and $\nu=0.38$, the differences in natural frequency for three models are large when the dimensionless thickness of the beam is small (e.g., $h/l<2$), whereas they are decreasing or even diminishing with the dimensionless thickness increasing. This indicates that the size effect is prominent only when the beam thickness is as small as the material length scale parameter. It is noted that the natural frequency with $\nu=0.0$ is always smaller than that with $\nu=0.38$ for the classical beam model. However, it is not true when $h/l<2.61$ for the present model and $h/l<1.37$ for the modified couple stress model. Therefore, Poisson effect on the natural frequency is more complicated than on the deflection and rotation in the static bending problem and will be discussed below.

The tendency of natural frequency predicted by the present model and the other two reduced Timoshenko beam models with Poisson's ratio are shown in Fig. 8, in which both cases of beam thickness $h=l$ and $h=2l$ are considered. It is observed that the natural frequency predicted by the modified couple stress model is smaller than that by the present model, while larger than that by the classical model with Poisson's ratio varying, which is consistent with that the present model exhibits increased bending rigidity, as

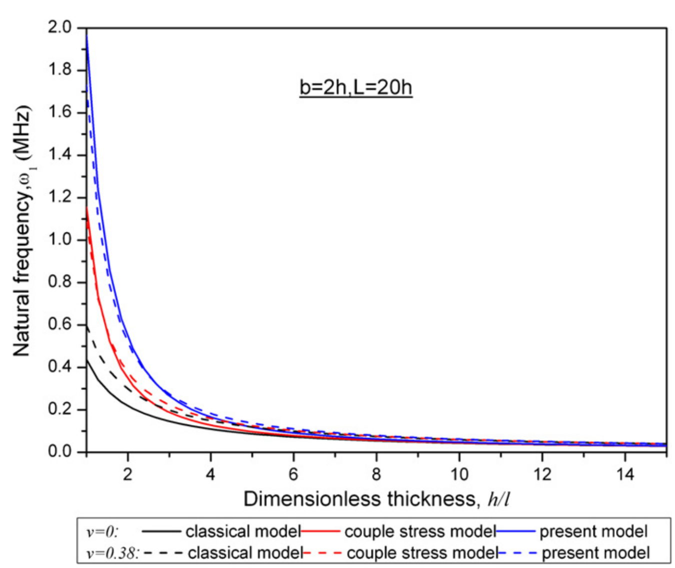

Fig. 7. Natural frequency varying with dimensionless thickness based on three different models with $\nu=0$, 0.38.

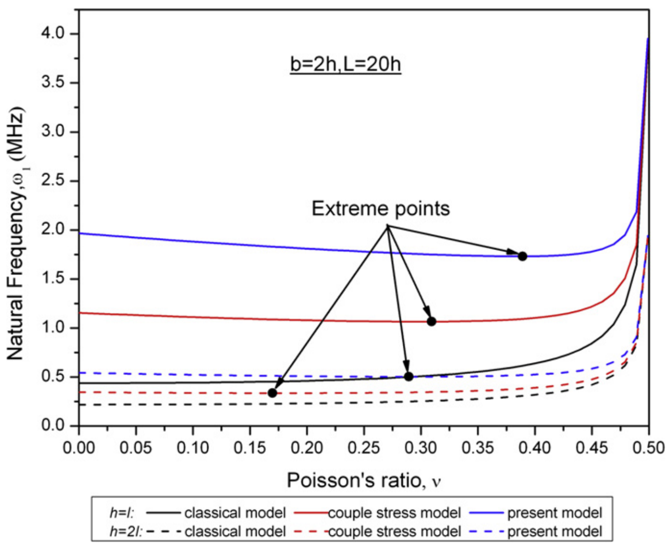

Fig. 8. Poisson effect on the natural frequency of the beam based on three different models with $h = l$, $2l$.

observed in static bending problem. It is also shown in Fig. 8 that results predicted by the present model and the modified couple stress model have minimum extreme points with Poisson's ratio increasing, indicating a similar "extreme point" phenomenon for the natural frequency as for the maximum deflection and rotation in Figs. 5 and 6. Meanwhile, it is observed that each Poisson's ratio where the minimum value of natural frequency occurs in Fig. 7 corresponds to that where the maximum deflection and maximum rotation occurs in Figs. 5 and 6, due to the fact that larger deflection results in smaller natural frequency and vice versa.

5. Conclusions

A micro scale Timoshenko beam model is developed based on strain gradient elasticity theory and Hamilton's principle. The new model incorporated with Poisson effect can capture the size effect due to containing material length scale parameters. Moreover, the model can reduce to the modified couple stress Timoshenko beam model or even the classical Timoshenko beam model. In addition, the newly developed model can also degenerate into the micro scale Bernoulli–Euler beam model based on strain gradient elasticity theory if shear deformation is ignored. Both static bending and free vibration problems of a simply supported beam are solved based on the currently developed model. Numerical results of the deflection, rotation and natural frequency predicted by the new model are compared with those by the modified couple stress Timoshenko beam model and the classical Timoshenko beam model with different conditions. The differences of results predicted by three models are quite large when the beam thickness is approximately as small as the material length scale parameter. These differences, however, are decreasing and diminishing with beam thickness increasing. Finally, Poisson effect on the results of static bending and free vibration problems possesses an interesting "extreme point" phenomenon, which is quite different from that predicted by the classical Timoshenko beam model.

Acknowledgements

The work reported here is funded by the National Natural Science Foundation of China (Grant No. 10572077), Specialized Research Fund for the Doctoral Program of Higher Education of China (Grant No. 20060422013) and the Natural Science Fund of Shandong Province of China (Grant No. Y2007F20).

References

Chasiotis, I., Knauss, W.G., 2003. The mechanical strength of polysilicon films: Part 2. Size effects associated with elliptical and circular perforations. Journal of the Mechanics and Physics of Solids 51, 1551–1572.
De Boer, M.P., Luck, D.L., Ashurst, W.R., et al., 2004. High-performance surface-micromachined inchworm actuator. Journal of Microelectromechanical Systems 13 (1), 63–74.
Dym, C.L., Shames, I.H., 1973. Solid Mechanics: A Variational Approach. McGraw-Hill Inc., New York.
Eringen, A.C., 1983. On differential equations of nonlocal elasticity and solutions of screw dislocation and surface waves. Journal of Applied Physics 54, 4703–4710.
Faris, W., Nayfeh, A.H., 2007. Mechanical response of a capacitive microsensor under thermal load. Communications in Nonlinear Science and Numerical Simulation 12 (5), 776–783.
Fleck, N.A., Hutchinson, J.W., 1993. Phenomenological theory for strain gradient effects in plasticity. Journal of Mechanics and Physics of Solids 41 (12), 1825–1857.
Fleck, N.A., Hutchinson, J.W., 1997. Strain gradient plasticity. Advances in Applied Mechanics 33, 296–358.
Fleck, N.A., Hutchinson, J.W., 2001. A reformulation of strain gradient plasticity. Journal of Mechanics and Physics of Solids 49 (10), 2245–2271.
Fleck, N.A., Muller, G.M., Ashby, M.F., Hutchinson, J.W., 1994. Strain gradient plasticity: theory and experiment. Acta Metallurgica et Materialia 42, 475–487.
Giannakopoulos, A.E., Stamoulis, K., 2007. Structural analysis of gradient elastic components. International Journal of Solids and Structures 44, 3440–3451.
Hall, N.A., Okandan, M., Degertekin, F.L., 2006. Surface and bulk-silicon-micromachined optical displacement sensor fabricated with the SwIFT-Lite process. Journal of Microelectromechanical Systems 15 (4), 770–776.
Heireche, H., Tounsi, A., Benzair, A., Maachou, M., Adda Bedia, E.A., 2008. Sound wave propagation in single-walled carbon nanotubes using nonlocal elasticity. Physica E 40, 2791–2799.
Hung, E.S., Senturia, S.D., 1999. Extending the travel range of analog-tuned electrostatic actuators. Journal of Microelectromechanical Systems 8 (4), 497–505.
Hutchinson, J.R., 2001. Shear coefficients for Timoshenko beam theory. ASME Journal of Applied Mechanics 68, 87–92.
Kaneko, T., 1975. On Timoshenko's correction for shear in vibrating beams. Journal of Physics D: Applied Physics 8, 1927–1936.
Kang, X., Xi, Z.W., 2007. Size effect on the dynamic characteristic of a micro beam based on cosserat theory. Journal of Mechanical Strength 29 (1), 1–4.
Kong, S.L., Zhou, S.J., Nie, Z.F., Wang, K., 2008a. The size-dependent natural frequency of Bernoulli–Euler micro-beams. International Journal of Engineering Science 46 (5), 427–437.
Kong, S.L., Zhou, S.J., Nie, Z.F., Wang, K., 2008b. Static and dynamic analysis of micro beams based on strain gradient elasticity theory. International Journal of Engineering Science 47, 487–498.
Lam, D.C.C., Chong, A.C.M., 1999. Indentation model and strain gradient plasticity law for glassy polymers. Journal of Materials Research 14, 3784–3788.
Lam, D.C.C., Yang, F., Chong, A.C.M., et al., 2003. Experiments and theory in strain gradient elasticity. Journal of Mechanics and Physics of Solids 51 (8), 1477–1508.
Lu, P., Lee, H.P., Lu, C., Zhang, P.Q., 2007. Application of nonlocal beam models for carbon nanotubes. International Journal of Solids and Structures 44, 5289–5300.
Ma, H.M., Gao, X.L., Reddy, J.N., 2008. A microstructure-dependent Timoshenko beam model based on a modified couple stress theory. Journal of Mechanics and Physics of Solids 56 (12), 3379–3391.
Maneschy, C.E., Miyano, Y., Shimbo, M., Woo, T.C., 1986. Residual-stress analysis of an epoxy plate subjected to rapid cooling on both surfaces. Experimental Mechanics 26, 306–312.
McFarland, A.W., Colton, J.S., 2005. Role of material microstructure in plate stiffness with relevance to micro cantilever sensors. Journal of Micromechanics and Microengineering 15, 1060–1067.
Mindlin, R.D., 1964. Micro-structure in linear elasticity. Archive for Rational Mechanics and Analysis 16 (1), 51–78.
Mindlin, R.D., 1965. Second gradient of strain and surface-tension in linear elasticity. International Journal of Solids and Structures 1 (1), 417–438.
Mindlin, R.D., Tiersten, H.F., 1962. Effects of couple-stresses in linear elasticity. Archive for Rational Mechanics and Analysis 11 (1), 415–448.
Moser, Y., Gijs, M.A.M., 2007. Miniaturized flexible temperature sensor. Journal of Microelectromechanical Systems 16 (6), 1349–1354.
Nix, W.D., 1989. Mechanical properties of thin films. Metallurgical and Materials Transactions A 20, 2217–2245.
Papargyri-Beskou, S., et al., 2003a. Dynamic analysis of gradient elastic flexural beams. Structural Engineering and Mechanics 15 (6), 705–716.
Papargyri-Beskou, S., et al., 2003b. Bending and stability analysis of gradient elastic beams. International Journal of Solids and Structures 40 (2), 385–400.
Park, S.K., Gao, X.L., 2006. Bernoulli–Euler beam model based on a modified couple stress theory. Journal of Micromechanics and Microengineering 16, 2355–2359.
Pei, J., Tian, F., Thundat, T., 2004. Glucose biosensor based on the microcantilever. Analytical Chemistry 76, 292–297.

Poole, W.J., Ashby, M.F., Fleck, N.A., 1996. Micro-hardness of annealed and work-hardened copper polycrystals. Scripta Materialia 34 (4), 559–564.
Salvetat, J.P., et al., 1999. Elastic and shear moduli of single-walled carbon nanotube ropes. Physical Review Letters 82 (5), 944–947.
Toupin, R.A., 1962. Elastic materials with couple-stresses. Archive for Rational Mechanics and Analysis 11 (1), 385–414.
Tsepoura, K.G., et al., 2002. Static and dynamic analysis of a gradient-elastic bar in tension. Archive of Applied Mechanics 72, 483–497.
Vardoulakis, I., Sulem, J., 1995. Bifurcation Analysis in Geomechanics. Blackie/Chapman & Hall, London.
Wang, C.M., 1995. Timoshenko beam-bending solutions in terms of Euler–Bernoulli solutions. ASCE Journal of Engineering Mechanics 121, 763–765.
Wang, Q., 2005. Wave propagation in carbon nanotubes via nonlocal continuum mechanics. Journal of Applied Physics 98 (124301), 1–6.
Wang, C.M., Zhang, Y.Y., Ramesh, S.S., Kitipornchai, S., 2006. Buckling analysis of micro- and nano-rods/tubes based on nonlocal Timoshenko beam theory. Journal of Physics D: Applied Physics 39, 3904–3909.
Wang, C.M., Zhang, Y.Y., He, X.Q., 2007. Vibration of nonlocal Timoshenko beams. Nanotechnology 18, 105401. 9pp.
Yang, F., Chong, A.C.M., Lam, D.C.C., et al., 2002. Couple stress based strain gradient theory for elasticity. International Journal of Solids and Structures 39 (10), 2731–2743.
Zhou, S.J., Li, Z.Q., 2001. Length scales in the static and dynamic torsion of a circular cylindrical micro-bar. Journal of Shandong University of Technology 31 (5), 401–407.